REPORT DOCUMENTATION PAGE

1. AGENCY USE ONLY (Leave blank)	2. REPORT DATE 20 December 1995	3. REPORT TYPE AND DATES COVERED Technical

4. TITLE AND SUBTITLE
SYNTHESIS, CHARACTERIZATION AND IMMOBILIZATION OF NANOCRYSTALLINE BINARY AND TERNARY III-V (13-15) COMPOUND SEMICONDUCTORS

5. FUNDING NUMBERS
- N00014-95-1-0194
  R&T Project 3135008---16
- Dr. Harold E. Guard

6. AUTHOR(S)
LARA I. HALAOUI, SHREYAS S. KHER, MICHAEL S. LUBE, STEVEN R. AUBUCHON, CAROLYNNE R. S. HAGAN, RICHARD L. WELLS*, AND LOUIS A. COURY*

7. PERFORMING ORGANIZATION NAME(S) AND ADDRESS(ES)

Department of Chemistry
Duke University
Durham, NC 27708-0346

8. PERFORMING ORGANIZATION REPORT NUMBER
Technical Report
No. DU/DC/TR-54

9. SPONSORING/MONITORING AGENCY NAME(S) AND ADDRESS(ES)

Office of Naval Research
300 North Quincy Street
Arlington, VA 22217-5000

10. SPONSORING/MONITORING AGENCY REPORT NUMBER

11. SUPPLEMENTARY NOTES

Accepted for Publication in *American Chemical Society Symposium Series*

DTIC
SELECTE
JAN 0 5 1996
F

12a. DISTRIBUTION/AVAILABILITY STATEMENT
Approved for Public Release
Distribution Unlimited

12b. DISTRIBUTION CODE

13. ABSTRACT (Maximum 200 words)

Two synthetic routes to nanocrystalline III-V (13-15) materials are discussed. The first employs dehalosilylation reactions between Group III trihalides and $E(SiMe_3)_3$ (E = P, As) om hydrocarbon solvents affording nanocrystalline III-V semiconductors or their precursors. The second involves reactions of MX_3 (M = Ga, X = Cl, I; M = In, X = Cl, I, in glymes with in situ synthesized $(Na/K)_3E$ (E = P, As, Sb) in aromatic solvents, yielding nanocrystalline GaP, GaAs, GaSb, InP, InAs, and InSb after refluxing reaction mixtures. Materials are characterized by TEM, XRD, Elemental Analysis, NMR, UV-vis, and STM. STM images of InAs give particle size distributions and confirm sample conductivity. Scanning tunneling spectroscopy shows a larger band gap for nanocrystalline InAs than for InAs wafers, consistent with quantum confinement.

19960104 231

14. SUBJECT TERMS Gallium, Phosphorus, Synthesis, Crystal Structure			15. NUMBER OF PAGES 21
			16. PRICE CODE

17. SECURITY CLASSIFICATION OF REPORT Unclassified	18. SECURITY CLASSIFICATION OF THIS PAGE Unclassified	19. SECURITY CLASSIFICATION OF ABSTRACT Unclassified	20. LIMITATION OF ABSTRACT Unlimited

SYNTHESIS, CHARACTERIZATION AND IMMOBILIZATION OF NANOCRYSTALLINE BINARY AND TERNARY III-V (13-15)COMPOUND SEMICONDUCTORS

LARA I. HALAOUI, SHREYAS S. KHER, MICHAEL S. LUBE,
STEVEN R. AUBUCHON, CAROLYNNE R. S. HAGAN,
RICHARD L. WELLS*, AND LOUIS A. COURY*

Duke University
Department of Chemistry,
P. M. Gross Chemical Laboratory
Box 90346
Durham, NC 27708-0346

20 December 1995

Synthesis, Characterization and Immobilization of Nanocrystalline Binary and Ternary III-V (13-15) Compound Semiconductors

L. I. Halaoui, S. S. Kher, M. S. Lube,
S. R. Aubuchon, C. R. S. Hagan,
R. L. Wells* and L. A. Coury, Jr.*

Department of Chemistry
Box 90346
Duke University
Durham, NC 27708-0346

Two synthetic routes to nanocrystalline III-V (13-15) materials are discussed. The first employs dehalosilylation reactions between Group III trihalides and $E(SiMe_3)_3$ (E = P, As) in hydrocarbon solvents affording nanocrystalline III-V semiconductors or their precursors. The second involves reactions of MX_3 (M = Ga, X = Cl, I; M = In, X = Cl, I) in glymes with in situ synthesized $(Na/K)_3E$ (E = P, As, Sb) in aromatic solvents, yielding nanocrystalline GaP, GaAs, GaSb, InP, InAs and InSb after refluxing reaction mixtures. Materials are characterized by TEM, XRD, Elemental Analysis, NMR, UV-vis, and STM. STM images of InAs give particle size distributions and confirm sample conductivity. Scanning tunneling spectroscopy shows a larger bandgap for nanocrystalline InAs than for InAs wafers, consistent with quantum confinement.

Much of the research interest in nanomaterials is attributable to the remarkably different properties displayed by these fascinating materials. For example, the prediction of size-dependent bandgaps for nanocrystalline semiconductors has excited speculation about their exploitation in novel optoelectronic and photoelectrochemical applications. Due to the relative ease with which they may be synthesized, most work to date has focused on metal nanoparticles and nanocrystalline II-VI (12-16) semiconductors. Despite the tremendous potential of unique properties and applications, however, nanocrystalline III-V (13-15) semiconductors remain largely unexplored. To this end, the work reported here details two different routes for the synthesis of nanocrystalline III-V materials, and discusses the characterization of these materials. In particular, it will be shown that stable, conductive, nanocrystalline materials with a reasonably narrow size distribution can be prepared which have a markedly different bandgap than commercial wafers of the bulk material.

Dehalosilylation as a Route to III-V (13-15) Compound Semiconductors

Introduction. Dehalosilylation (or silyl halide elimination) has come to the fore as a viable synthetic technique in main group chemistry. In 1986, we first reported the use of dehalosilylation as a means to the formation of Ga-As bonds (*1*). Since then, researchers in our laboratory (*2-8*) as well as numerous other investigators (*9-15*) have applied this method, or adaptations thereof, in the preparation of compounds containing bonds between elements of Group III and Group V, as well as III-V semiconductor materials. Buhro and coworkers have applied dehalosilylation in the formation of ternary II-IV-V materials, (*16*) and Cowley and coworkers have recently synthesized BiP through a dehalosilylation route (*17*). Research in our laboratory has focused on the preparation of single-source precursors to binary and ternary III-V materials utilizing primarily the dehalosilylation method. However, Alivisatos and co-workers (*15*) observed that nanocrystalline GaAs was obtainable from the 1:1 mole ratio reaction of $GaCl_3$ and $As(SiMe_3)_3$ in solution, a reaction originally reported from our laboratories (*18-19*). Therefore, closer examination of the materials derived from the thermolyses of our III-V precursors was warranted.

Binary III-V Investigations: Precursors and Nanocrystalline Materials. We have reported the syntheses and characterization of a new class of dimeric species containing four-membered ring cores of alternating gallium and phosphorus atoms, with all exocyclic ligands on the metal centers being halogens; *viz.*, $[X_2GaP-(SiMe_3)_2]_2$ (X = Cl, Br, I) (*7-8*). These dimers were prepared from the 1:1 mole ratio reaction of GaX_3 with $P(SiMe_3)_3$, resulting in the elimination of one molar equivalent of Me_3SiX to yield the dimeric complex. Subsequent thermolysis of these dimers at 400 °C resulted in the elimination of the remaining Me_3SiX, yielding powders containing nanocrystalline GaP of 3 nm average domain size (*8*).

Also reported were novel precursors of formula $(Ga_2ECl_3)_n$ (E = P, As) which result from the separate 2:1 mole ratio reactions of $GaCl_3$ with either $P(SiMe_3)_3$ (*7*) or $As(SiMe_3)_3$ (*20*). These powders undergo $GaCl_3$ elimination at temperatures > 300 °C to produce nanocrystalline GaP (*7*) or GaAs (*21*) (domain size *ca.* 3 nm). Structural data on the precursors are unavailable, however, as both have been found to be highly insoluble in hydrocarbon solvents.

Initial research on the reactions of $InCl_3$ with $As(SiMe_3)_3$ showed the 1:1 mole ratio reaction to proceed directly to crystalline InAs, however neither the size of the crystallites nor the effect of using a different indium(III) halide was determined (*18-19*). Subsequent research to investigate these points indicated that all 1:1 mole ratio reactions of InX_3 (X = Cl, Br, I) produce a black or brown-black powder, which upon annealing at 400 °C gives nanocrystalline InAs (characterized by XRD, XPS, TEM, and elemental analysis) with domain sizes ranging from 9-12 nm (*22*). When $InCl_3$ was allowed to react with $As(SiMe_3)_3$ in a 2:1 mole ratio reaction in an attempt to isolate a compound similar to the aforementioned $(Ga_2ECl_3)_n$, a red-brown powder resulted. This powder was not found to have the expected 3:2:1 ratio of Cl:In:As, however it did eliminate a yellow powder upon thermolysis (presumably $InCl_3$) at 400 °C to yield nanocrystalline InAs of 16 nm domain size (*22*).

Barron and coworkers originally investigated the 1:1 mole ratio reactions of InX_3 (X = Cl, Br, I) with $P(SiMe_3)_3$, yielding insoluble powders which were identified by elemental analysis to be oligomeric species of formula $[X_2InP(SiMe_3)_2]_n$ (14,23). Upon thermolysis, these powders were found to decompose to crystalline InP, however particle sizes of these samples were not reported. Further investigation of these reactions in our laboratories revealed that these powders progressed to nanocrystalline InP upon thermolysis at 400 °C, with domain sizes around 3 nm (22). Also, the 1:1 mole ratio reaction of InI_3 with $P(SiMe_3)_3$ was found to yield the 1:1 Lewis acid-base adduct $I_3In\cdot P(SiMe_3)_3$. This compound was found by TGA to eliminate three molar equivalents of Me_3SiI to yield nanocrystalline InP (identified by XRD, XPS, TEM, and elemental analysis), of domain size 2 nm (22).

Ternary III-V Investigations. The focus in our laboratories has recently been expanded to include investigations into ternary III-V compounds and materials. Dehalosilylation has proven an effective pathway to both precursors and materials with ternary formulations, whether the target compound contains two different group III elements and a pnicogen, or one group III element and two pnicogens.

As mentioned earlier, the 2:1 reaction of $GaCl_3$ with $E(SiMe_3)_3$ produced an oligomeric precursor compound $(Ga_2ECl_3)_n$ which upon thermolysis eliminated $GaCl_3$ to produce nanocrystalline GaE (E = P, As) (8, 20-21). Since either pnicogen can be used to synthesize a compound of formula $(Ga_2ECl_3)_n$, it seemed possible that a mixture of $P(SiMe_3)_3$ and $As(SiMe_3)_3$ could react with $GaCl_3$ in a 2:1 metal:pnicogen ratio to produce a similar mixed-pnicogen precursor of formula $[Ga_2(P/As)Cl_3]_n$. An off-white, insoluble powder was isolated from such a reaction and identified by elemental analyses as this mixed-pnicogen oligomer. Thermolysis of $[Ga_2(P/As)Cl_3]_n$ at 400 °C resulted in elimination of $GaCl_3$ and subsequent formation of a dark brown powder. This powder was confirmed by XRD, XPS, and elemental analyses to be the ternary III-V semiconductor $GaAs_xP_y$ (0.6 ≤ x,y ≤ 0.9) (21). Furthermore, X-ray powder diffraction studies of the $GaAs_xP_y$ showed the powder to be nanocrystalline, with domain size of ca. 3 nm. The reflections observed in this pattern fall between those expected for GaAs (24) and GaP (25), which would be expected according to Vegard's Law (26-27), further confirming the identity of this mixed-pnicogen semiconductor.

Based on the success of the 2:1 mole ratio metal:pnicogen mixed-pnicogen reaction described above, several 1:1 mole ratio metal:pnicogen preparations were investigated in order to synthesize mixed-pnicogen ring complexes or to develop routes to mixed-metal or mixed-pnicogen ternary materials. A Ga-As-Ga-P ring compound,

$\overline{I_2GaAs(SiMe_3)_2Ga(I)_2}P(SiMe_3)_2$, had previously been synthesized in our laboratories through equilibration of its constituent dimeric complexes $[I_2GaE(SiMe_3)_2]_2$ (E = P, As) (28) and seemed to be a good candidate for synthesis by a more direct method. To this end, GaI_3, $As(SiMe_3)_3$, and $P(SiMe_3)_3$ were allowed to react in solution in a 2:1:1 mole ratio to produce a yellow powder which was fully characterized as being

$\overline{I_2GaAs(SiMe_3)_2Ga(I)_2}P(SiMe_3)_2$ (29). This compound was thermolyzed at 400 °C,

and observed both in bulk decomposition and TGA studies to eliminate four molar equivalents of Me_3SiI to produce $GaAs_xP_y$ as a brown-black powder. XRD studies of this powder (Figure 1A) displayed the (111) peak between the expected values for GaAs (24) and GaP (25) (Table I), which by Vegard's Law (26-27) is evidence for the presence of $GaAs_xP_y$ in the sample. However, due to the small particle size of the crystallites (domain size ca. 1 nm) the (220) and (311) peaks were broadened such that they could not be easily identified. Thus, an additional sample of the cyclic precursor was heated at 450 °C for 12 hours. The resulting brown powder was shown to be $GaAs_xP_y$ of 2.4 nm particle size, with the three major peaks in the XRD being readily identifiable (see Table I). Elemental analysis of the $GaAs_xP_y$ powder obtained at 400 °C showed x = 0.65 and y = 0.52, with significant contamination by C, H, and I.

Table I. Comparison of Prepared Ternary III-V Materials with JCPDS Files for Binary III-V Materials (d-spacings in angstroms).

	(111)	(220)	(311)
GaAsP			
GaAs standard (24)	3.26	2.00	1.70
GaAsP sample (400 °C)	3.24	N/A[a]	N/A[a]
GaAsP sample (450 °C)	3.21	1.97	1.70
GaP standard (25)	3.14	1.92	1.64
GaInP			
GaP standard (25)	3.14	1.92	1.64
GaInP sample	3.18	(1.98)[b]	(1.68)[b]
InP standard (30)	3.39	2.08	1.77
InAsP			
InP standard (30)	3.39	2.08	1.77
InAsP sample	3.46	2.12	1.81
InAs standard (31)	3.50	2.14	1.83

[a] Data inconclusive: line-broadening due to small particle size obscured these peaks.

[b] Line broadening due to small particle size results in poor signal-to-noise ratio; values obtained from a compressed spectrum.

Similar direct preparations using different metal/pnicogen combinations have resulted in insoluble powders which were found to decompose to a ternary material. The reaction of a solution-phase mixture of $GaCl_3$ and $InCl_3$ with two molar equivalents of $P(SiMe_3)_3$ resulted in a light yellow powder with a Ga:In:P ratio of 1.04:1.00:1.05, however no crystalline sample suitable for single-crystal X-ray analysis could be obtained, nor could a compound be identified from these data.

Thermolysis of this powder at 400 °C yielded a brown powder with a Ga:In:P ratio of 2.69:1.00:4.16, and significant C, H, and Cl contamination. An XRD pattern of this sample (Figure 1B) showed it to be nanocrystalline (domain size *ca.* 1 nm), with (111), (220) and (311) reflections located between those expected for GaP (*25*) and InP (*30*) (Table I), indicative of the presence of a ternary GaInP mixed-metal semi-conductor in the powder sample.

A similar one-pot synthesis was also conducted in an attempt to form the ternary mixed-pnicogen semiconductor InAsP. Two molar equivalents of $InCl_3$ were allowed to react in solution with a mixture of one molar equivalent each of $As(SiMe_3)_3$ and $P(SiMe_3)_3$, yielding a brown powder with an In:As:P ratio of 3.71:1.85:1.00. Once again, no crystalline sample could be obtained from this powder. Subsequent thermolysis of this sample at 400 °C yielded a lustrous black powder with a In:As:P ratio of 2.38:1.89:1.00. The XRD pattern of this sample (Figure 1C) also showed it to be nanocrystalline (domain size *ca.* 9 nm), with (111), (220) and (311) reflections located between those expected for InP (*30*) and InAs (*31*) (Table I), again indicative of the presence of a ternary semiconductor, InAsP. A high-resolution TEM image of this sample (Figure 2) shows lattice planes for several nanocrystalline InAsP particles ranging in size from 6 to 15 nm.

Although the current results from preparations of ternary materials utilizing the silyl cleavage method are preliminary, the aforementioned data has encouraged further investigation into synthesizing precursors to III-V ternary and quaternary materials using this versatile reaction pathway.

Synthesis of III-V Semiconductor Nanocrystals by Solution Phase Metathesis

Introduction. We have recently published a straightforward new method for preparing nanocrystalline III-V semiconductors (*32-34*). This method utilizes *in situ* reactions of Group III halides in chelating solvents with $(Na/K)_3E$ (E = P, As, Sb) in aromatic solvents. Semiconductor nanocrystallites with average particle size of 4-35 nm can be prepared using this method and GaP (diameter = 11 nm), GaAs (10 nm), GaSb (35 nm), InP (4 nm), InAs (11 nm) and InSb (26 nm) have each been obtained. The particle sizes of the semiconductors depend on the nature of Group III halide, nature of the solvent, concentration and chain length of the glyme solvents used. When $GaCl_3$ was dissolved in various solvents and subsequently reacted with $(Na/K)_3As$, synthesized *in situ* in refluxing toluene, different average particle sizes of GaAs were obtained: toluene (36 nm), dioxane (36 nm), monoglyme (17 nm) and diglyme (10 nm). The chelating nature of multi-dentate glyme solvents seem to play a crucial role in limiting the growth of GaAs crystallites beyond a certain size. It was also observed that dimeric Group III halides ($GaCl_3$, GaI_3 and InI_3) gave final products with much smaller particle sizes. Oligomeric $InBr_3$ and $InCl_3$, on the other hand, gave nanocrystallites with larger particle size.

Characterization and Surface Chemistry. Thus obtained quantum crystallites have been characterized by various techniques. Figure 3 shows a high resolution transmission electron micrograph (HRTEM) of GaP nanocrystallites. Numerous lattice fringes

originating from 3-12 nm crystallites are observed in the figure. The XRD pattern indicated that the average particle size of this GaP sample was 11 nm (*32*). Our earlier reports (*32-34*) dealt with particles from which excess Group V element was sublimed away. Currently we have focused on nanocrystallites in the as-prepared state, *i.e.*, obtained by simply refluxing the reaction mixture. The as-prepared GaAs nanocrystallites have been investigated in great detail (*35*). These materials are quite interesting since they are capped and can form remarkably stable colloidal suspensions without requiring any surfactants. For example, upon repeated extractions of as-synthesized GaAs with methanol, grey colloidal suspensions are formed which have been stable for more than 16 months despite repeated exposure to atmosphere and light.

These capped GaAs nanoclusters present in the colloid have been characterized by XRD, multi-nuclear NMR, HRTEM, XPS, FT-IR photoacoustic spectroscopy (PAS), Elemental Analysis, UV-Vis and atomic force microscopy (AFM) (*35*). FT-IR PAS, NMR and XPS analysis showed that the GaAs particles were capped by methanol used during the extractions, and no other impurities were detected. FT-IR PAS and NMR indicated that methanol and the residual water in the methanol were molecularly bound to the nanocrystal surface, and features assignable to dissociative binding of methanol and water were not observed. The hydrogen bonding between surface-bound and free solvent molecules in the colloid is a likely cause of the remarkable stability of these GaAs suspensions.

The average crystallite size of the particles obtained by evaporating methanol from the colloid was 5 nm. HRTEM of the solids from the grey colloid showed lattice planes due to 3-11 nm particles, although majority of the particles were 4-8 nm as evident from the fringe patterns. Figure 4 shows HRTEM images of GaAs quantum dots in the grey colloid. The micrograph shows several crystallites clustered together due to solvent evaporation from the colloid; however, due to methanol capping, the nanocrystals exist in the colloid in an isolated state as observed in AFM studies (*36*). Centrifugation of the grey colloid at 1315 G force for 30 min resulted in settling of larger crystallites and a reddish-orange colloid was obtained. HRTEM of the solids in the reddish-orange colloid showed that it mostly contained crystallites smaller than 2 nm, and larger crystallites such as those seen in Fig. 4 were not present in this colloid.

The XRD pattern of the particles in the reddish-orange colloid was inconclusive as it showed two broad humps. Crystallites smaller than ~3 nm do not yield conclusive diffraction pattern and appear to be "XRD amorphous" (*37-38*). Previously we have reported lattice fringe patterns from crystallites as small as 1 nm (*32*). The UV-Vis spectrum of the reddish-orange colloid showed rise in absorption at ~510 nm. The ^{71}Ga NMR of this colloid showed that it contained GaAs (*39*). When several drops of reddish-orange colloid were placed on a glass slide and the solvent was allowed to evaporate, orange GaAs particles were obtained. The as-prepared grey colloidal suspensions contain GaAs nanocrystals with a wide particle size distribution. Fischer, *et al.*, have recently used size exclusion and hydrodynamic chromatography techniques to separate nanocrystalline particles by size (*40*) and these techniques will be explored in future studies to obtain monodisperse crystallites and probe their properties.

Characterization of Nanocrystalline InAs Prepared by Solution Phase Metathesis and Dehalosilylation Reactions Using Scanning Tunneling Microscopy (STM) and Spectroscopy (STS)

Background Information. Nanocrystalline semiconductor materials are increasingly being suggested as possible components for new electro-optical devices (*41*). The number of experimental reports in which electrical characterization has been attempted on these systems, however, is quite limited (*42*). Aside from estimates of band gaps from absorbance measurements (*15,43,44*), very little data have appeared to date for materials other than II-VI compounds (*45*). Because of the relative purity and stability of our III-V materials (*8,18-22*), however, such investigations are now feasible. Preliminary data from scanning tunneling microscopy (STM) and scanning tunneling spectroscopy (STS) experiments are thus reported below for nanocrystalline InAs samples.

STM and STS are two members of a family of characterization techniques capable of providing information about conductive samples with nanometer resolution (*46*). In STM, an extremely sharp electrode called a "tip" is positioned within a few nanometers of a conductive sample. A small dc-potential (50 - 100 mV) called the "bias voltage" is applied between the tip and surface, which induces a tunneling current. An image may then be obtained by moving the tip in the x-y plane above the sample by plotting the fluctuations in tunneling current as a function of position ("constant height mode"). Alternatively, the value of the tunneling current can be fixed via electronic feedback, causing the tip to move in the z-direction at each (x,y) position to re-establish the desired current. This method is referred to as the "constant current mode," and was employed for the studies reported below. The images shown thus represent the tip displacement (z-coordinate) for each location in the x-y plane.

The STS technique is useful for probing the electronic properties of a sample (*45*). In the implementation used here, the tip is held over a single (or possibly several) semiconductor particle(s) while the bias voltage is swept over a range of potentials. The tunneling current is then monitored as a function of the bias voltage value to give information about the location of the semiconductor band edges. For example, the region along the potential axis where very little tunneling current is monitored can be used to estimate the band gap of the sample.

Characterization Methods. Measurements were made with a Digital Instruments NanoScope II using Pt-Ir or electrochemically-etched W tips (*42*). Diglyme-capped, nanocrystalline InAs particles prepared using the solution metathesis reaction, as well as InAs from the dehalosilylation synthetic route, were deposited from sonicated, methanol suspensions onto polycrystalline Pt or Au electrodes. These electrodes were obtained commercially (AAI-AbTech) and were prepared by magnetron sputtering onto borosilicate glass. STM images were obtained in air using the constant current mode of the instrument, typically with bias voltages in the range 50-100 mV at a set-point current of 1.2 nA with 400 samples per scan.

STS measurements were made on InAs samples using silicone oil as a bathing fluid. Various other liquids were examined as alternatives (*e.g.*, methanol, diglyme) but only silicone oil allowed for STS scans without dislodging the particles. The typical voltage range used was ± 1.1 to 1.4 V to maintain tunneling currents during scanning to less than ± 50 nA. The experiment was implemented by positioning the tip using a 0.4 V bias at a set-point current of 1.5 nA. Comparison data were obtained for freshly etched, single crystal Zn-doped *p*-InAs wafers, which had been passivated by treatment with a sodium sulfide solution. Evaporated films of Au (1350 Å) over Zn (153 Å) provided ohmic back contact to the wafers for these investigations.

Representative Data. Figure 5 shows an STM image of InAs particles deposited onto a Pt electrode. (For comparison, an image of the featureless, bare Pt surface is shown in Figure 6.) The particles appear fairly uniform in size, and are surprisingly evenly dispersed across the surface. The lack of aggregation seen may, in fact, be due to the diglyme capping agents, which also allow for the particles to form methanol suspensions which are stable for months.

The fact that an image was obtainable for nanocrystalline InAs suggests that it is sufficiently conductive to support a substantial tunneling current in the as-prepared state (*i.e.*, without deliberate doping). We have routinely been able to obtain STM images for the nanocrystalline III-V materials we have prepared by both the solution metathesis and dehalosilylation synthetic routes (*vide supra*). This includes data for nanocrystalline GaAs, a material with a substantially larger bandgap and lower intrinsic conductivity (47). However, in the case of nanocrystalline GaAs, a much larger bias voltage is needed to obtain an image (*circa* 2.0 V compared to 52 mV for this image of InAs), consistent with the different electronic properties of GaAs.

By taking sequential cross-sections of images such as the one shown in Figure 5, it is possible to obtain a particle size distribution for the nanocrystals. Figure 7 shows one such distribution, in this case revealing an arithmetic mean diameter of 14 nm with a sample standard deviation of 5 nm for a sample comprised of 124 particles. The best-fit gaussian function for the histogram shown was:

$$y = (-0.933) + (37.1)e^{\left(-0.5 \left(\frac{x-15.2}{5.72} \right)^2 \right)}$$

giving a coefficient of determination (R^2) of 0.981, and a centroid of 15.2 nm. Since the exciton diameter for InAs is estimated to be 62.5 nm (22), this particular sample should exhibit quantum confinement effects (*e.g.*, a larger band gap than bulk InAs).

STS experiments were subsequently performed to investigate this possibility. Representative results are shown in Figure 8, comparing data for nanocrystalline InAs with that for a wafer of single crystal *p*-InAs. As is evident, the "zero-current" region is noticeably larger for the InAs particles, demonstrating a larger band gap. It is important to note that this measurement probes the band gap of one (or a few) particle(s). This is in contrast to techniques such as photoluminescence,

XRD, BET or absorption spectroscopy which yield a composite (weighted-average) value. Furthermore, STS is not subject to the effects of photon scattering (42), since it is a "dark" or ground-state measurement.

To assess the precision of the STS experiments, replicate measurements were made for both the nanocrystalline material and the sulfide-passivated single crystal wafer. The mean band gap taken from 38 experiments (with each experiment representing the average of 40 current measurements at each voltage) on a sulfide-passivated p-InAs wafer was found to be 0.41 eV with a sample standard deviation of 0.08 eV. This agrees (within experimental error) with the literature value of 0.36 eV for non-passivated InAs. By contrast, 21 measurements on the nanocrystalline InAs material yielded a mean band gap value of 0.837 eV with a sample standard deviation of 0.126 eV. The greater amount of scatter in the latter data set is entirely expected, since a distribution in particle sizes (and hence band gaps) exists for the sample (cf., Figure 7). We have previously published the UV/vis absorption spectrum for a methanol suspension of nanocrystalline InAs prepared by the dehalosilylation method (22), and that spectrum showed an absorption edge which was severely blue-shifted (λ = 322 nm) relative to that expected for bulk InAs (3444 nm). Thus, these STS data are consistent with the spectroscopic results, and confirm the presence of quantum confinement effects in nanocrystalline InAs.

Acknowledgments

Literature Cited

(1)   Pitt, C. G.; Purdy, A. P.; Higa, K. T.; Wells, R. L. *Organometallics* **1986**, *5*, 1266.

(2)   Wells, R. L. *Coord. Chem. Rev.* **1992**, *112*, 273, and references therein.

(3)   Wells, R. L.; Jones, L. J.; McPhail, A. T.; Alvanipour, A. *Organometallics* **1991**, *10*, 2345.

(4)   Wells, R. L.; McPhail, A. T.; Speer, T. M. *Organometallics* **1992**, *11*, 960.

(5)   Wells, R. L.; McPhail, A. T.; Jones, L. J.; Self, M. F. *Polyhedron* **1993**, *12*, 141.

(6)   Jones, L. J.; McPhail, A. T.; Wells, R. L. *Organometallics* **1994**, *13*, 3634.

(7)   Wells, R. L.; Self, M. F.; McPhail, A.T.; Aubuchon, S. R.; Woudenberg, R. C.; Jasinski, J. D. *Organometallics* **1993**, *12*, 2832.

(8)   Aubuchon, S. R.; McPhail, A. T.; Wells, R. L.; Giambra, J. A.; Bowser, J. B. *Chem. Mater.* **1994**, *6*, 82.

(9) Uchida, H.; Matsunga, T.; Yoneyama, H.; Sakata, T.; Mori, H.; Sasaki, T. *Chem. Mater.* **1993**, *5*, 716.

(10) Stuczynski, S. M.; Opila, R. L.; Marsh, P.; Brennan, J. G.; Steigerwald, M. L. *Chem. Mater.* **1991**, *3*, 379.

(11) Douglas, T.; Theopold, K. H. *Inorg. Chem.* **1991**, *30*, 594

(12) Butler, L.; Redmond, G.; Fitzmaurice, D. *J. Phys. Chem.* **1993**, *97*, 10750.

(13) Mićić, O. I.; Curtis, C. J.; Jones, K. M.; Sprague, J. R.; Nozik, A. J. *J. Phys. Chem.* **1994**, *98*, 4966.

(14) Healy, M. D.; Laibinis, P. E.; Stupik, P. D.; Barron, A. R. *J. Chem. Soc. Chem. Commun.* **1989**, 359.

(15) Olshavsky, M. A.; Goldstein, A. N.; Alivisatos, A. P. *J. Am. Chem. Soc.* **1990**, *112*, 9438.

(16) Goel, S. C.; Buhro, W. E.; Adolphi, N. L.; Conradi, M. S. *J. Organomet. Chem.* **1993**, *449*, 9.

(17) Carmalt, C. J.; Cowley, A. H.; Hector, A. L.; Norman, N. C.; Parkin, I. V. *J. Chem. Soc. Chem. Commun.* **1994**, 1987.

(18) Wells, R. L.; Pitt, C. G.; McPhail, A. T.; Purdy, A. P.; Shafie-ezad, S.; Hallock, R. B. *Chem. Mater.* **1989**, *1*, 4.

(19) Wells, R. L.; Pitt, C. G.; McPhail, A. T.; Purdy, A. P.; Shafie-ezad, S.; Hallock, R. B. *Mater. Res. Soc. Symp. Proc.* **1989**, *131*, 45.

(20) Wells, R. L.; Hallock, R. B.; McPhail, A. T.; Pitt, C. G.; Johansen, J. D. *Chem. Mater.* **1991**, *3*, 381.

(21) Aubuchon, S. R.; Lube, M. S.; Wells, R. L. *Chem. Vap. Deposition* **1995**, *1*, 28.

(22) Wells, R. L.; Aubuchon, S. R.; Kher, S. S.; Lube, M. S.; White, P. S. *Chem. Mater.* **1995**, *7*, 793.

(23) Healy, M. D.; Laibinis, P. E.; Stupik, P. D.; Barron, A. R. *Mater. Res. Soc. Symp. Proc.* **1989**, *131*, 83.

(24) *Joint Committee on Powder Diffraction Standards (JCPDS)*, File No. 14-450, GaAs.

(25) *JCPDS*, File No. 12-191, GaP.

(26) Cullity, B. D. *Elements of X-Ray Diffraction, 2nd edn.*; Addison-Wesley: Reading, MA, 1978; pp 375-377.

(27) Wiley, J. B.; Kaner, R. B. *Science* **1992**, *255*, 1093.

(28) Wells, R. L.; McPhail, A. T.; White, P. S.; Lube, M. S.; Jones, L. J. *Phosphorus, Sulfur, and Silicon* **1994**, *93-94*, 329.

(29) Wells, R. L.; Aubuchon, S. R.; Lube, M. S. *Main Group Chemistry* **1995**, *1*, 81.

(30) *JCPDS*, File No. 13-232, InP.

(31) *JCPDS*, File No. 15-869, InAs.

(32) Kher, S. S.; Wells, R. L. *Chem. Mater.* **1994**, *6*, 2056.

(33) Kher, S. S.; Wells, R. L. *Mater. Res. Soc. Symp. Proc.* **1994**, *351*, 293.

(34)   Kher, S. S.; Wells, R. L. *U. S. Patent* Application No. 08/189,232.

(35)   Kher, S. S.; Wells, R. L. *to be published.*

(36)   Falvo, M.; Superfine, R.; Kher, S. S.; Wells, R. L. *to be published.*

(37)   Herron, N.; Wang, Y.; Eckert, H. *J. Am. Chem. Soc.* **1990**, *112*, 1322.

(38)   Murray, C. B.; Norris, D. J.; Bawendi, M. G. *J. Am. Chem. Soc.* **1993**, *115*, 8706.

(39)   Potter, L.; Wu, Y.; Kher, S. S.; Wells, R. L. *to be published.*

(40)   Fischer, Ch.-H.; Giersig, M. *J. Chromatogr. A* **1994**, *688*, 97, and references therein.

(41)   Meyer, G. J.; Searson, P. C. *Electrochem. Soc. Interface* **1993**, *2*, 23.

(42)   Hagan, C. R. S.; Kher, S. S.; Halaoui, L. I.; Wells, R. L.; Coury, L. A., Jr. *Anal. Chem.* **1995**, *67*, 528.

(43)   Uchida, H.; Curtis, C. J.; Nozik, A. J. *J. Phys. Chem.* **1991**, *95*, 5382.

(44)   Mićić, O. I.; Sprague, J. R.; Curtis, C. J.; Jones, K. M.; Machol, J. L.; Nozik, A. J.; Giessen, H.; Fluegel, B.; Mohs, G.; Peyghambarian, N. *J. Phys. Chem.* **1995**, *99*, 7754.

(45)   Ogawa, S.; Fan, F.-R. F.; Bard, A. J. *J. Phys. Chem.* **1995**, *99*, 11182.

(46)   Christmann, K. *Introduction to Surface Physical Chemistry*; Springer-Verlag: New York, 1991; pp 102-107.

(47)   Solymar, L.; Walsh, D. *Lectures on the Electrical Properties of Materials, 4th edn.*; Oxford: New York, 1990.

Figure 1. XRD Powder Patterns of Ternary III-V Materials Prepared by Dehalosilylation.

Figure 2. High-Resolution TEM of InAsP Nanocrystals.

Figure 3. High-Resolution TEM of GaP Nanocrystals. The bar in the figure indicates a scale of 6 nm.
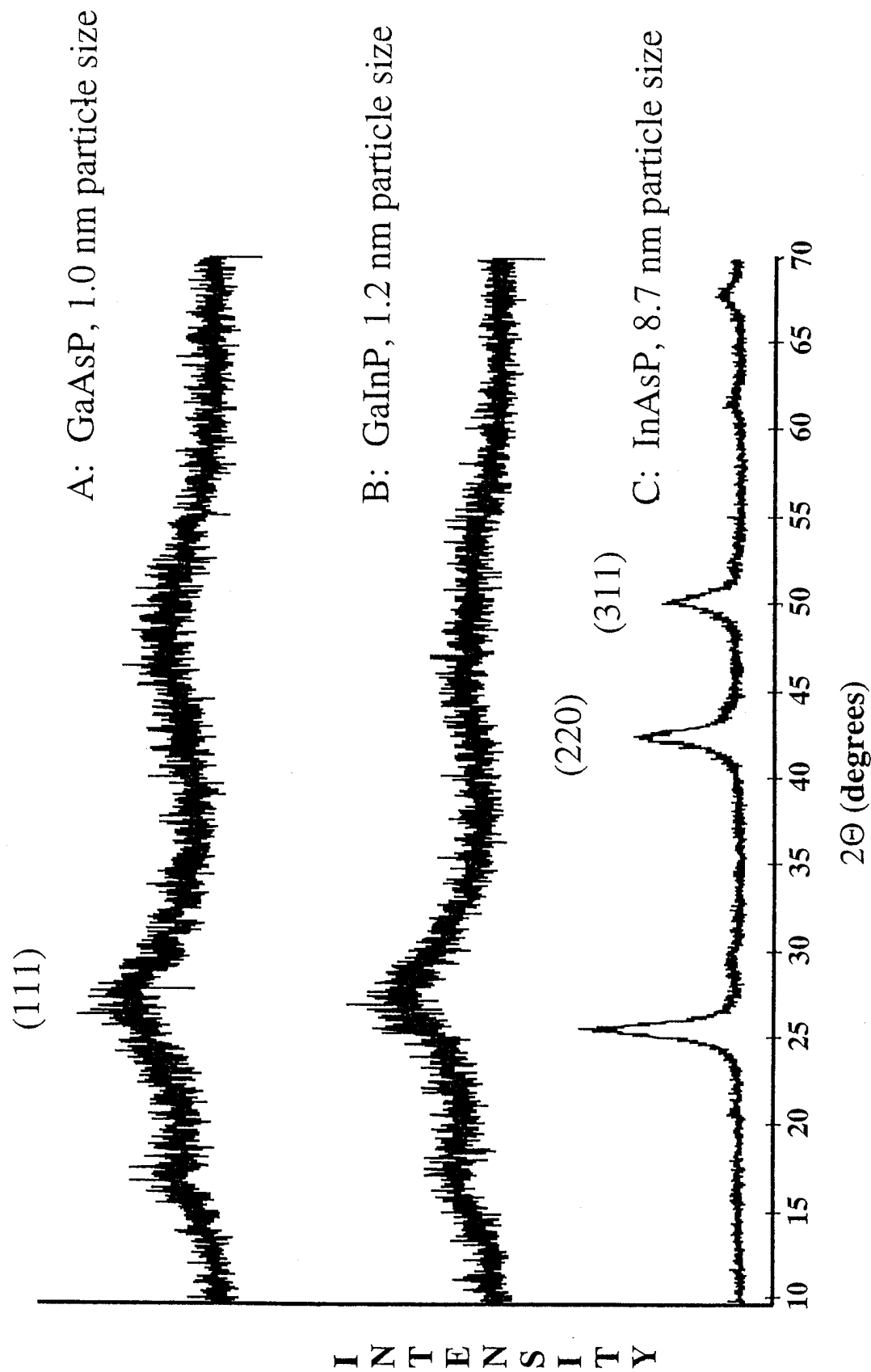
Figure 4. High-Resolution TEM of GaAs quantum dots obtained from evaporating solvent from the grey colloidal suspension. The image shows several crystallites clustered together due to solvent evaporation. The bar indicates a scale of 7 nm.
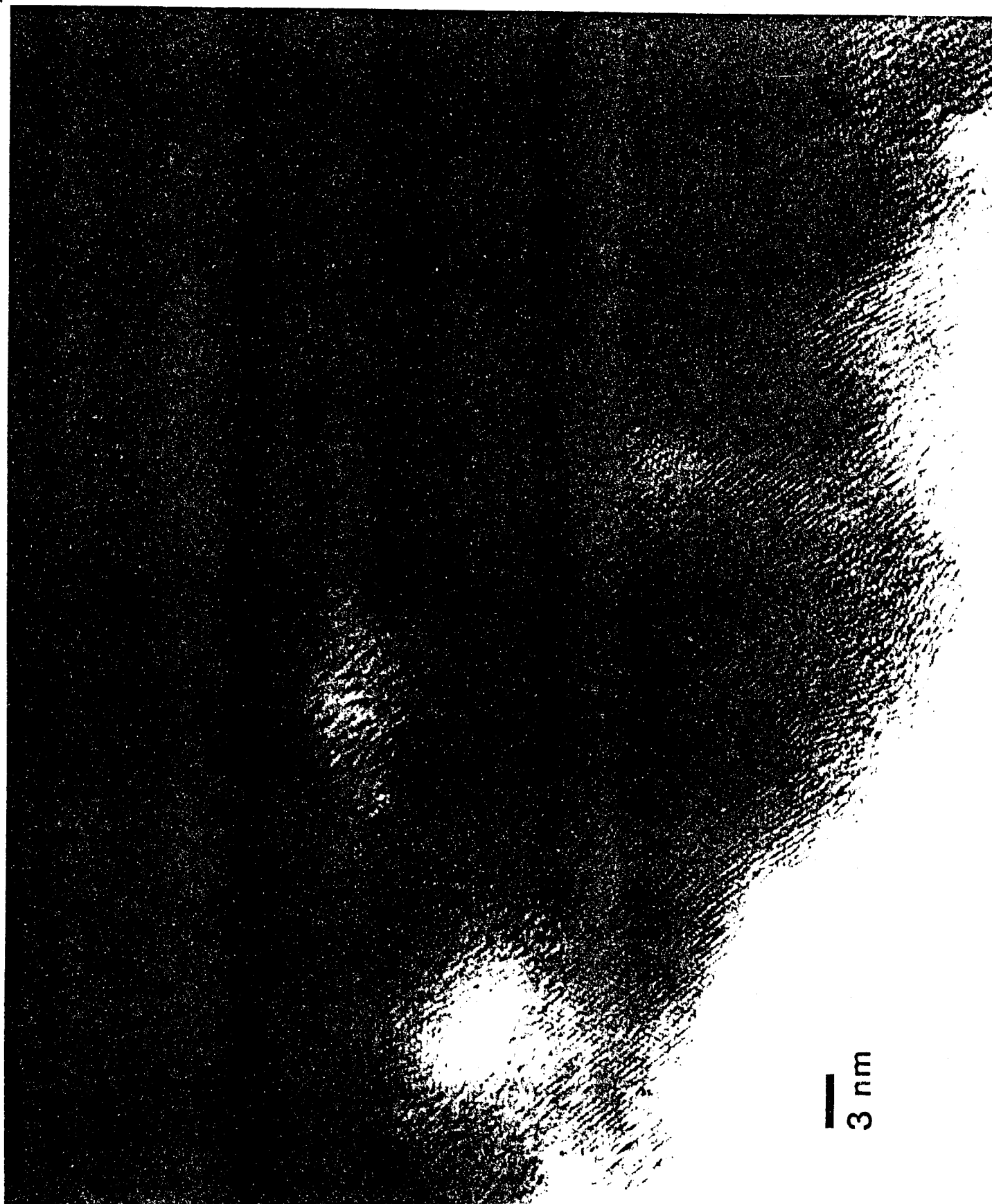
Figure 5. STM of InAs Nanocrystals deposited on Pt substrate. *Panel A:* top view; *Panel B:* side view.

Figure 6. STM of bare Pt substrate electrode.

Figure 7. Particle size distribution obtained from cross-sections of STM image.

Figure 8. STS plots comparing data for nanocrystalline InAs (Δ) with that for a wafer of single-crystal p-InAs ($+$).
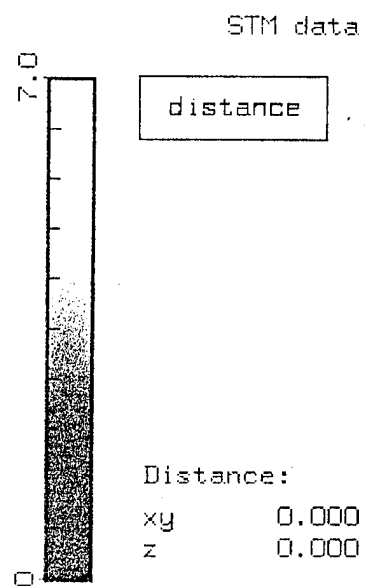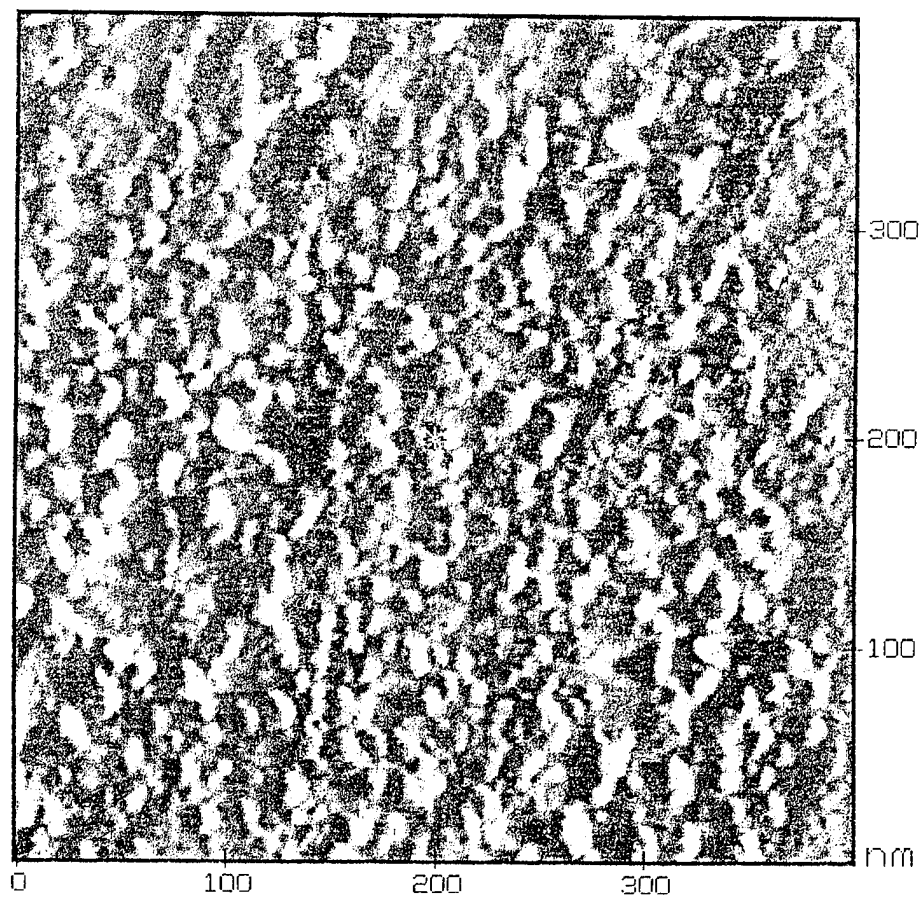
A: GaAsP, 1.0 nm particle size

B: GaInP, 1.2 nm particle size

C: InAsP, 8.7 nm particle size

(111)

(220)

(311)

2Θ (degrees)

INTENSITY

3 nm

6 nm

7nm

STM data

distance

Distance:
xy   0.000
z   0.000

Nanoscope II
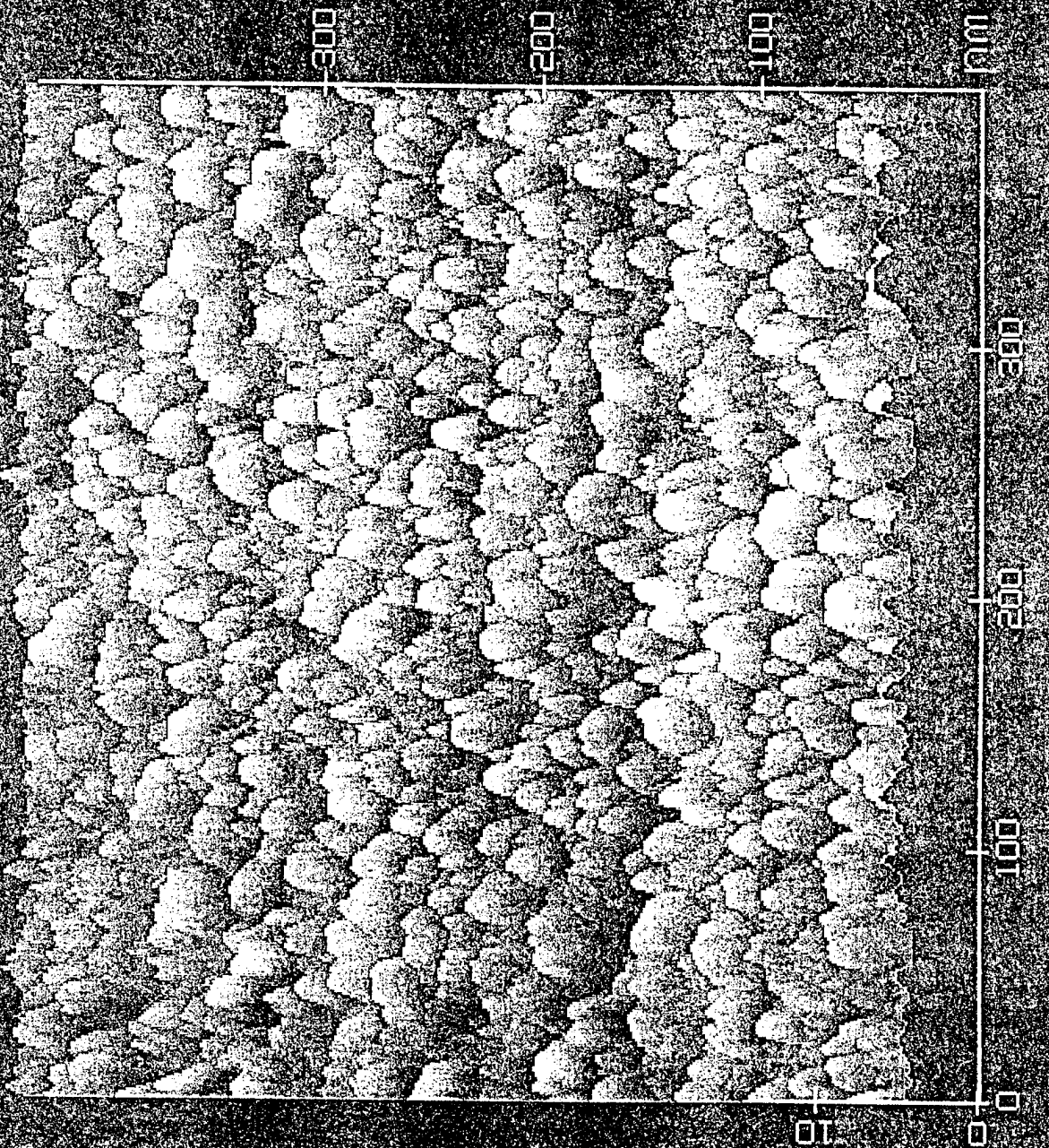Parameters:

Bias   51.9 mV
Setpoint   1.2 nA
Z   5.1 Å/ln(I)
XY   19.6 Å/V
Samples   400/scan

Data taken Wed Jun 08 14:34:27 1994
Buffer 2(PTINAS.11(F)), Rotated 0°, XY axes [nm], Z axis [nm]
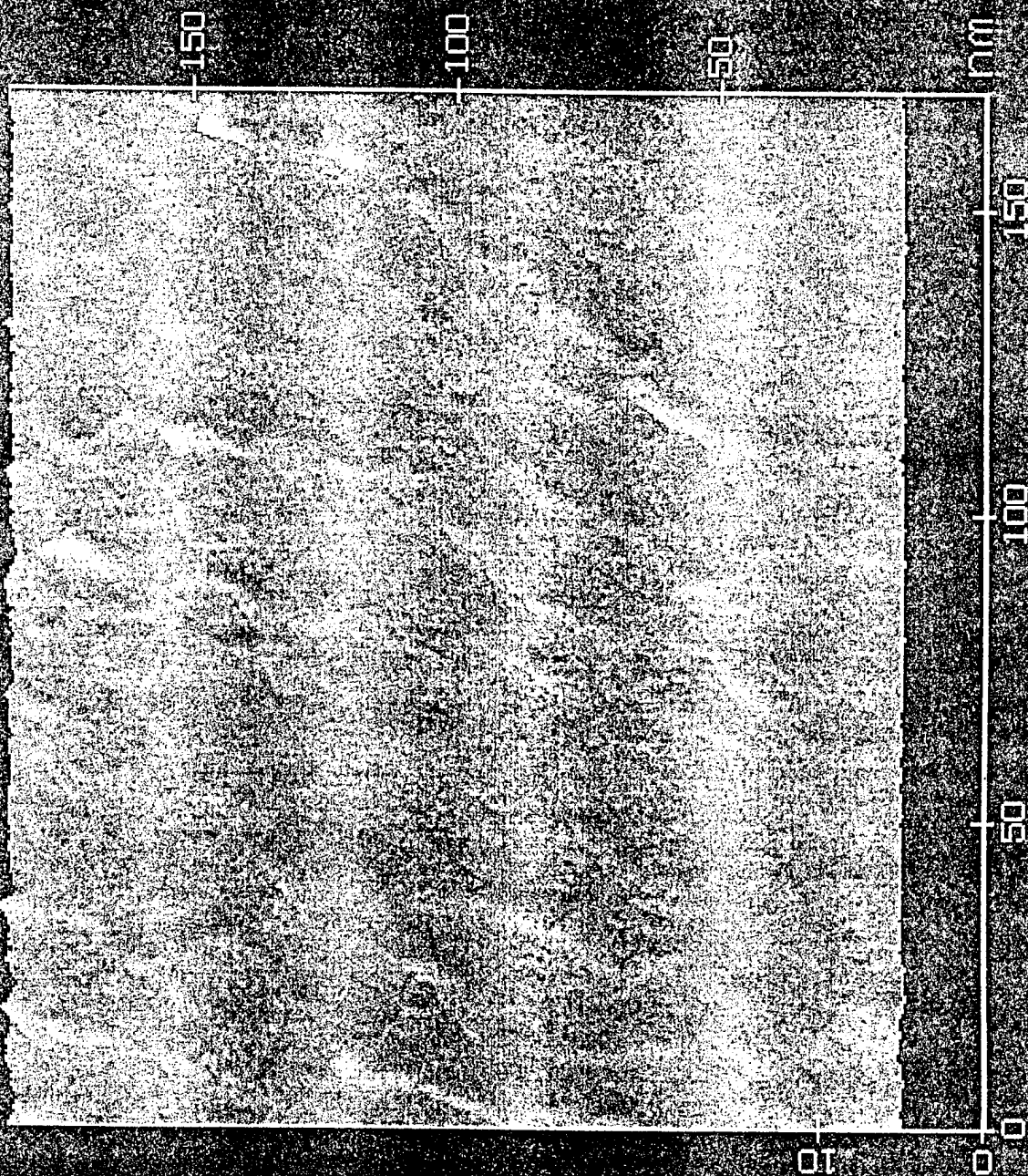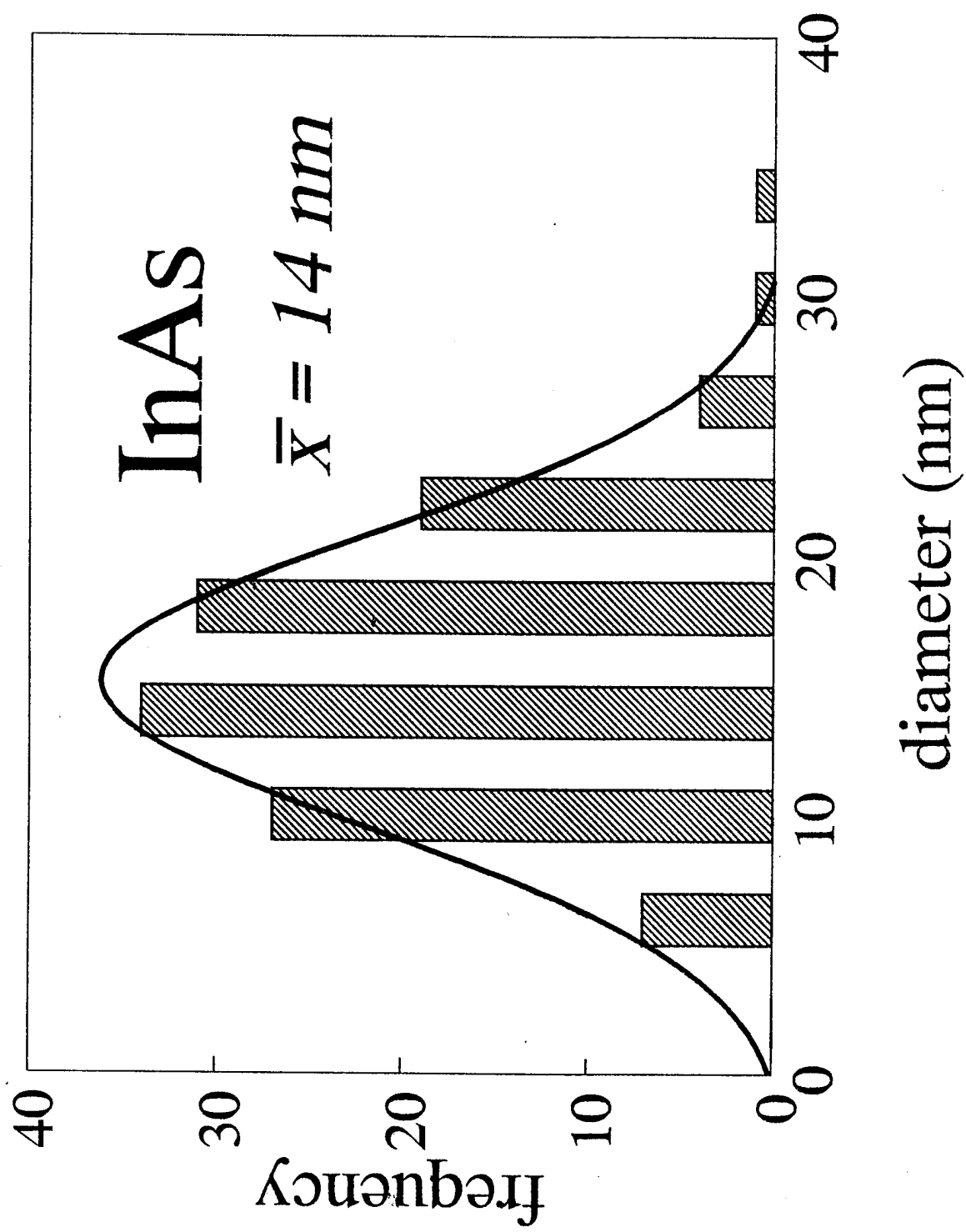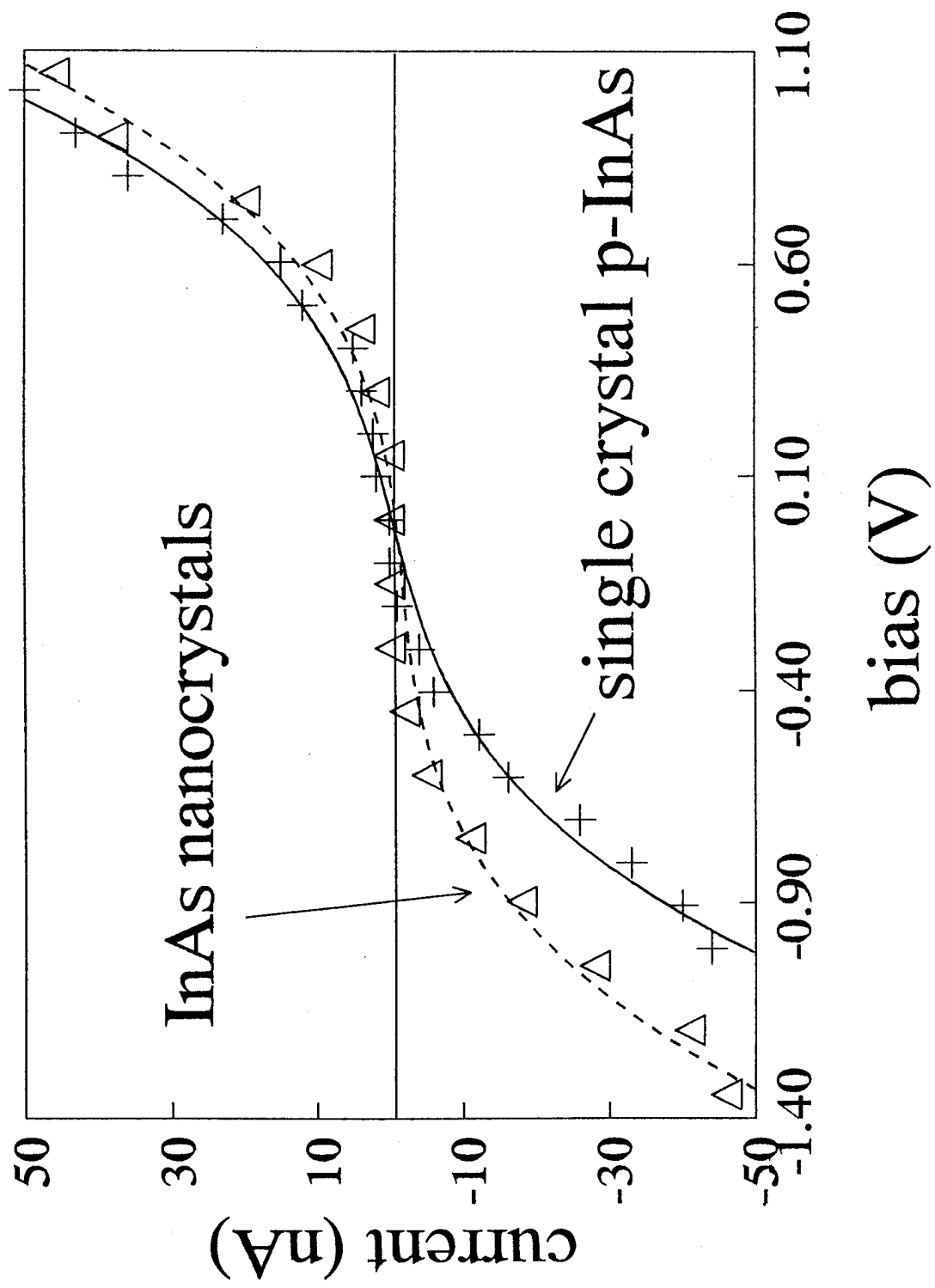
STM data

Nanoscope II
Parameters:

Bias   80.0 mV
Setpoint   2.0 nA
Z   5.1 Å/in(I)
N XY   19.6 Å/O
Samples   400/scan

nm XY

Data taken Wed May 04 13:37:17 1994
Buffer 4(PTO.006(F)), Rotated 0°, XY axes [nm], Z axis [nm]

InAs

$\overline{X} = 14\ nm$

diameter (nm)

frequency

TECHNICAL REPORT DISTRIBUTION LIST - GENERAL

Office of Naval Research   (1)*
Chemistry Division, ONR 331
800 North Quincy Street
Arlington, Virginia 22217-5660

Defense Technical Information
   Center   (2)
Building 5, Cameron Station
Alexandria, VA 22314

Dr. James S. Murday   (1)
Chemistry Division, Code 6100
Naval Research Laboratory
Washington, D.C. 20375-5320

Dr. John Fischer, Director   (1)
Chemistry Division, C0235
Naval Air Weapons Center
  Weapons Division
China Lake, CA 93555-6001

Dr. Peter Seligman   (1)
Naval Command, Control and
  Ocean Surveillance Center
RDT&E Division
San Diego, CA 92152-5000

Dr. Richard W. Drisko   (1)
Naval Facilities & Engineering
 Service Center
Code L52
Port Hueneme, CA 93043

Dr. Eugene C. Fischer   (1)
Code 2840
Naval Surface Warfare Center
  Carderock Division Detachment
Annapolis, MD 21402-1198

Dr. Bernard E. Douda   (1)
Crane Division
Naval Surface Warfare Center
Crane, Indiana 47522-5000

* Number of copies to forward